

1-D Mott insulator transition of a Bose-Einstein condensate

R. E. Sapiro, R. Zhang, G. Raithel

FOCUS Center and Department of Physics, University of Michigan

(Dated: August 30, 2021)

The superfluid to one-dimensional Mott-insulator transition of a ^{87}Rb Bose-Einstein condensate is demonstrated. In the experiment, we apply a one-dimensional optical lattice, formed by two laser beams with a wavelength of 852 nm, to a three dimensional BEC in a shallow trap. We use Kapitza-Dirac scattering to determine the depth of the optical lattice without knowledge of its exact geometry. We further study the dynamics of the transition as well as steady-state phase behavior specific to the one-dimensional case.

PACS numbers: 03.75.Lm,37.10.Jk,67.85.Hj

Bose-Einstein condensation (BEC) was first demonstrated in 1995 [1, 2], creating an explosion of interest in previously unattainable many-body quantum phenomena. Of particular interest is the phase transition from superfluid to Mott insulator [3]. In the general, three-dimensional (3-D) case, this phase transition occurs when a 3-D optical lattice is applied to a BEC. As the lattice depth is increased, the BEC transitions from a superfluid state to a state with a definite number of atoms in each lattice well. The Mott insulator transition has drawn the interest of both atomic and condensed matter physicists, due to the possibilities it creates for simulating ideal, controlled condensed matter systems. Under the correct circumstances the transition could be used to create supersolids or other novel phases of matter [4]. Doping the Mott insulator with fermions can be used to simulate a semiconductor [5]. One can use Feshbach resonances to create molecules in a Mott insulator with two atoms per site [6], which could eventually lead to a molecular BEC [7, 8]. The Mott insulator state could also provide a means to entangle neutral atoms and form a quantum register for a quantum computer (for a review, see Ref. [9]). Several laboratories have succeeded in producing the transition from a BEC to a 3-D Mott insulator [3, 5, 6, 10]. In lower dimensions, the Mott insulator transition has been achieved using 2-D [11, 12] and 1-D [13] Bose gases. One of the difficulties in attaining the Mott insulator transition is that the lattice depth necessary to induce the transition requires high laser power or, more commonly, narrowly focused beams. Demonstrating the transition from a BEC to a 1-D Mott insulator (a 3-D BEC in a 1-D lattice formed by two laser beams) is even more difficult because a deeper lattice is needed [14, 15]. Furthermore, it can be difficult to determine the exact lattice depth due to uncertainties in the lattice beam alignment. In this paper, we experimentally investigate the properties of Mott insulator transition of a 3-D BEC in a 1-D lattice using a novel, robust method to calibrate the lattice depth. In contrast to Ref. [13], we apply no transverse lattice potential [16]. The quantum gas therefore retains superfluidity in the two dimensions transverse to the lattice-beam direction, with observable consequences.

In the experiment, we start with a ^{87}Rb BEC of 5×10^4

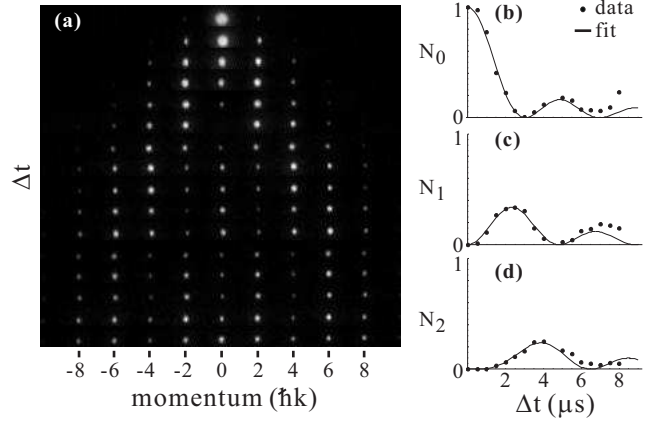


FIG. 1: (a) TOF images of Kapitza-Dirac scattering as a function of lattice duration Δt , in steps of $0.5 \mu\text{s}$, starting from $0.5 \mu\text{s}$. (b)-(d) Scattering ratios N_n/N_T , as defined in the text, for the scattering orders $n = 0, 1$, and 2 , respectively, as a function of lattice duration. The data in (b) are fit with $J_0^2(a\Delta t)$, with best-fit parameter $a=0.79$. The lines in (b)-(d) show $J_n^2(0.79\Delta t)$ with respective values of n .

8×10^4 atoms in a practically harmonic magnetic trap. Our BEC apparatus is described in [17]. In the data presented, we use magnetic-trap frequencies of 80 Hz and 200 Hz in the direction of the optical lattice (in the other two directions, the trap frequencies are 20 Hz and 80 Hz or 40 Hz and 200 Hz, respectively). The optical lattice is formed by a retro-reflected, far-off-resonance laser beam (wavelength 852 nm, power up to 200 mW after fiber). The beam is focused into a spot with an intensity full-width half-maximum of $80 \mu\text{m}$. The depth of the optical lattice is obtained as follows.

When a standing wave of sufficiently short duration is applied to cold atoms such that the atoms are stationary while the lattice is applied, the system is in the Kapitza-Dirac scattering regime (analogous to the Raman-Nath regime in optics). The 1-D optical lattice adds a potential

$$V(x) = -V_0(1 - \cos(2k_L x)) \quad (1)$$

to the atoms over the time interval Δt that the lattice is on. $2V_0$ is the lattice depth, and k_L is the wavenumber of the lattice beams. Assuming an initial wavefunction

$\psi(x, t = 0) = 1$, the wavefunction after the lattice pulse is, neglecting a global phase factor,

$$\begin{aligned} \psi(x, t > 0) &= \exp\left(i \frac{V_0 \Delta t \cos(2k_L x)}{\hbar}\right) \\ &= \sum_{n=-\infty}^{\infty} (i)^n J_n\left(\frac{V_0 \Delta t}{\hbar}\right) \exp(i2nk_L x). \end{aligned} \quad (2)$$

The expression in the sum shows that the BEC breaks up into momentum components that are integer multiples of $2\hbar k_L$ with amplitudes given by Bessel functions. In particular, the order $n = 0$ first vanishes at a time Δt_0 for which $V_0 = 2.4048\hbar/\Delta t_0$. The lattice depth $2V_0$ can thus be found by measuring the time Δt at which the $n = 0$ order first vanishes. For an atomic polarizability α and a single-beam lattice intensity I_1 , the lattice depth is also given by $2V_0 = \alpha I_1 / (2c\epsilon_0)$. Using the above equations, the lattice depth can be experimentally calibrated against arbitrary linear functions of I_1 , such as the measured beam power. The strength of this method is that no geometrical measurements of the lattice beam size and position are necessary.

To examine the Kapitza-Dirac scattering, the optical lattice is applied to the BEC for a few microseconds. The lattice and the trap are then turned off simultaneously. The BEC is allowed to expand freely for times of flight (TOF) of 16 ms or 12 ms, for the case of the 80 Hz or 200 Hz traps, respectively. After the expansion, we take absorption images, shown in Fig. 1 (a). Since the BEC temperature depends on the trap frequency, different trap frequencies require different TOFs to produce the best image. For each scattering order n , we measure the atom number N_n (N_T is the total atom number). In Fig. 1 (b) we plot N_0/N_T vs Δt and find the lattice duration Δt_0 where this ratio first approaches zero; the corresponding lattice depth is $4.8096\hbar/\Delta t_0$. In this way, we can determine the proportionality constant relating the lattice-power reading to the lattice depth. Typically, we find $\Delta t_0 \sim 3 \mu\text{s}$, which is well within the validity range of the short-pulse approximation underlying the above treatment, as evidenced by the fits in Fig. 1 (b) which match the data well up to $6 \mu\text{s}$. In the measurements presented this paper, this calibration procedure is repeated frequently to account for small changes in the alignment of the lattice beams. Furthermore, this procedure is used to initially align the lattice with respect to the BEC: better overlap between the lattice and the BEC leads to a smaller Δt_0 .

With the lattice depth calibrated, we investigate the transition from a superfluid to a 1-D Mott insulator. While in Kapitza-Dirac scattering a sudden, microsecond pulse is applied, the transition of the BEC from a superfluid to a Mott insulator requires adiabatic loading of the atoms into the optical lattice, taking of order ten milliseconds. We use the amplitude modulation of an AOM to control the power of our lattice beam. We ramp up the power of the lattice beam from zero to its final value over 10 ms, and then hold it there for 5 ms.

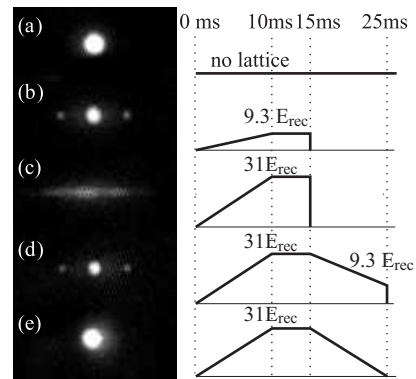


FIG. 2: Left: TOF images. Right: lattice depth as a function of time for (a) BEC with no lattice, (b) superfluid phase, (c) 1-D Mott insulator, (d) superfluid phase recovered after Mott insulator, and (e) BEC with no lattice, recovered after Mott insulator.

Then, we simultaneously turn off the lattice and the magnetic trap, and take a TOF measurement. As can be seen in Fig. 2 (b), for small lattice depths the BEC is only slightly modulated by the lattice, corresponding to the appearance of only two weak side peaks, at $\pm 2\hbar k_L$. As the depth of the lattice is increased, the transition to Mott insulator occurs. The typical signature of the transition is that the side peaks disappear and the central peak broadens, reflecting the momentum distribution of the localized wavefunction in a single lattice well [3]. Here, we find that the system fully reaches the 1-D Mott insulator state around $30 E_{\text{rec}}$.

The Mott insulator transition is a quantum phase transition, and thus is reversible; to be certain that we have seen the Mott transition, as opposed to a lattice-induced heating effect, we must show that we can reverse it. To demonstrate this, we ramp the lattice to $31 E_{\text{rec}}$ over 10 ms, hold it there for 5 ms, and then ramp back down over 10 ms. As can be seen in Figs. 2 (d) and (e), we obtain a modulated superfluid and BEC when we ramp down to a weak lattice and no lattice, respectively. Thus, the effect we see is fully reversible, providing strong evidence that it is the 1-D Mott insulator transition.

In the 1-D Mott-insulating state (Fig. 2 (c)), the quantum gas loses phase coherence in the direction of the optical lattice while retaining its superfluidity in the other two directions. The 1-D Mott insulator can thus be thought of as a stack of uncorrelated pancake BECs, each containing ~ 3000 atoms under the conditions of Fig. 2 (c). As can be seen in Fig. 2 (c), the 1-D Mott insulator expands much farther in the direction of insulation than in the directions of superfluidity. This is largely due to the momentum spread of the pancake BECs in the lattice-beam direction. Examining the TOF image in Fig. 2 (c), we find a velocity spread of $\Delta p/m_{\text{Rb}} = 8 \text{ mm/s}$. Using the Heisenberg uncertainty relation, $\Delta x \Delta p \geq \hbar/2$, this corresponds to a localization $\Delta x = 46 \text{ nm}$, or 11% of the lattice period. Neglect-

ing mean-field effects and using the fact that the lattice wells are approximately harmonic near their minima, we find an oscillation frequency of $2\pi \times 35$ kHz for a lattice with a depth of $30 E_{\text{rec}}$, and velocity and position uncertainties of 8.9 mm/s and 41 nm, respectively, for the ground state. These numbers match the values derived from Fig. 2 (c) quite well, showing that the expansion in the lattice-beam direction is mostly driven by the kinetic energy of the pancake BECs in the optical-lattice wells.

A more subtle effect is that in the insulating case the expansion transverse to the lattice-beam direction is considerably slower than in the lattice-free BEC: about 1.5 mm/s and 2.5 mm/s, respectively. We attribute the difference to a variation in the manifestation of the repulsive mean-field potential (estimated to be $\lesssim 1$ kHz for our BECs in 200 Hz magnetic traps). Without the lattice, the BEC expansion is driven by a combination of the mean-field pressure and the kinetic energy of the BEC in the magnetic trap, leading to a final expansion speed of about 2.5 mm/s in all directions in Fig. 2 (a). After application of the deep, Mott-insulating lattice in Fig. 2 (c), the expansion is mostly driven by the comparatively high kinetic energy of the BEC pancakes in the optical-lattice wells, leading to a much faster expansion in the lattice direction. The faster expansion leads to a reduction of the time over which a substantial mean-field pressure exists, leading to a reduced final expansion speed transverse to the lattice, as observed.

To quantitatively characterize the 1-D Mott transition, we examine it as a function of lattice depth. We use the visibility of the side peaks, v , to map out the transition:

$$v = \frac{N_A - N_B}{N_A + N_B} \quad (3)$$

where N_A is the linear atom density of one side peak, and N_B is the linear atom density at the minimum between the center peak and the side peak. The timing of the lattice application is as described above. Examining the resulting image, we take the linear atom density as a function of position in the lattice direction along the central strip of the image, integrating over three pixels in height (a pixel in the image corresponds to $6.7 \mu\text{m}$). For N_A , we choose the local maximum at the side peak, if there is one, and for N_B we choose the local minimum between the side peak and the central peak, as shown in the sample data in Fig. 3 (a). If there is no local side maximum, we designate $v = 0$. We calculate the visibility separately for the side peaks on the left and right, and repeat the calculation for five separate images at each lattice depth. We then average the ten resulting values to get the visibility plotted in Fig. 3 (b). As can be seen, the Mott transition starts around $10 E_{\text{rec}}$, where v first reaches a value lower than its initial value. The BEC has fully transitioned to the Mott insulator state by $30 E_{\text{rec}}$, where $v = 0$. Our system contrasts strongly with that of a 1-D Bose gas, where the Mott transition is complete around $10 E_{\text{rec}}$ [13]. In 3-D, the Mott transition is complete around $20 E_{\text{rec}}$ [3]. This is in general

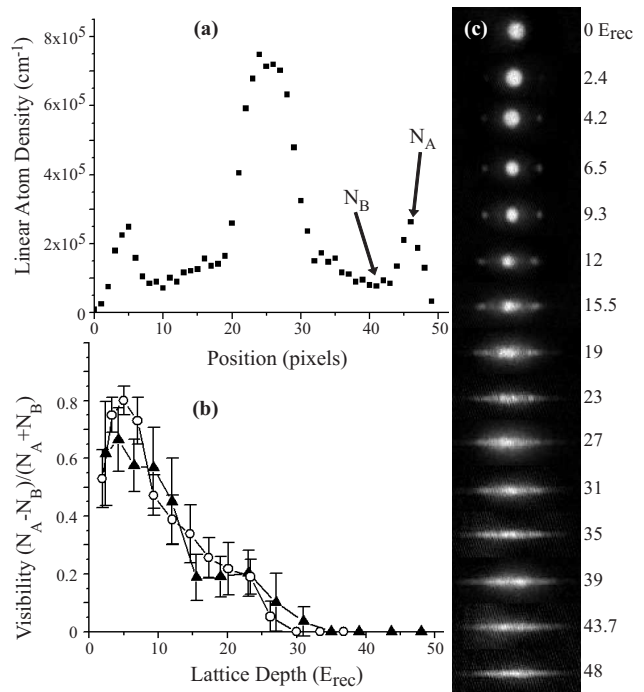


FIG. 3: (a) Linear atom density distribution for a BEC after 12 ms TOF, released from a lattice with a depth of $9.3 E_{\text{rec}}$ and magnetic trap with 200 Hz frequency. N_A is the height of the side peak and N_B is the height of the valley. (b) Visibility as a function of lattice depth from a 80 Hz magnetic trap (circles) and a 200 Hz trap (triangles). (c) TOF images as a function of lattice depth for a 200 Hz magnetic trap.

accordance with the prediction in Ref. [14] that the 1-D Mott transition requires a deeper lattice than the 3-D Mott transition. The specifics do not match, however, in that the lattice depth predicted in Ref. [14] necessary for the Mott transition is upwards of $50 E_{\text{rec}}$ for a system like ours with $\sim 3,000$ atoms per lattice well. As can be seen in Fig. 3 (b), the Mott transition happens under the same lattice conditions in the 80 Hz trap and the 200 Hz trap. This indicates that at both 80 Hz and 200 Hz the trap has no noticeable effect compared to the lattice.

Ideally, the visibility should be unity until the Mott transition starts [18]. In the experiment, however, even a minute thermal background will lower the visibility, and will disproportionately affect images with lower N_A . As $N_A, N_B \rightarrow 0$, this will prevent the visibility in Eq. 3 from reaching unity. For these reasons, the first few data points in Fig. 3 (b) not only fail to approach unity, but are even lower than visibilities seen for lattice depths $\sim 5 E_{\text{rec}}$. We are, however, confident that these issues do not affect our determination of where the Mott insulator transition occurs, because the transition happens at a lattice depth where both N_A and N_B are large.

When the lattice is ramped up, the pancake BECs in the individual lattice wells maintain a global phase until the Mott insulator transition is reached. Even beyond that point, the pancake BECs in their separate wells re-

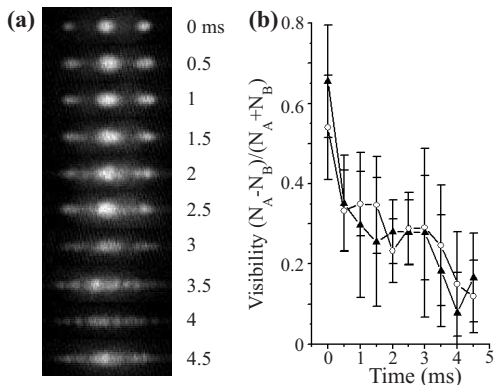


FIG. 4: (a) TOF images as a function of holding time in a lattice of $23 E_{\text{rec}}$ depth in a 200 Hz magnetic trap. (b) Visibility as a function of holding time of the lattice, for an 80 Hz magnetic trap (circles) and a 200 Hz trap (triangles).

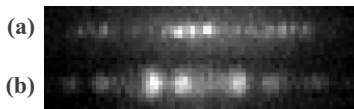


FIG. 5: TOF images of Mott insulators from magnetic traps with frequencies (a) 80 Hz and (b) 200 Hz. The speckles vary from shot to shot, and are due to interference during TOF of pancake BECs from different lattice wells.

quire a certain time to entirely dephase with respect to each other; only after the dephasing can one see the typical signatures of the Mott insulator transition (for example, in Fig. 3 (c) for lattices of depths larger than about $20 E_{\text{rec}}$). For deeper lattices, the time needed to dephase is too short to observe. Within the range of the superfluid to 1-D Mott insulator transition, however, the dephasing time can become sufficiently long to be observable. To measure the dephasing time, we start by ramping the lattice over 10 ms to $23 E_{\text{rec}}$, leave the lattice on for a variable hold time, and take TOF images as a function of the hold time, as shown in Fig. 4 (a). The visibilities in Fig. 4 (b) are obtained as described above. In the case of Fig. 4, the dephasing takes of order three milliseconds.

In many of the images of the Mott insulator, bright

and dark vertical stripes appear. These stripes can be seen in nearly all of the images of the Mott insulator from the 80 Hz trap, and several, but not all, of the Mott insulator images from the 200 Hz trap. For example, in Fig. 3 (c), the stripes are visible in the images at 23 and $35 E_{\text{rec}}$. The arrangement of the stripes appears random, with no repetition of the pattern from image to image, but the characteristic size of the stripes remains the same for a given magnetic trap frequency. We believe that these stripes represent interference between pancake BECs from different lattice wells during TOF. In the 1-D Mott insulator state, each pancake BEC still has a definite, but random phase. During TOF, the pancakes all expand into each other, leading to a characteristic interference speckle size. In Fig. 5 we show interference patterns in TOF images for the two different magnetic trap depths. To find the characteristic speckle size, Δs , in these images, we take fast Fourier transforms (FFT) of five images and average them for each trap depth. The value of Δs is given by the inverse spatial frequency where the FFT signal reaches the noise floor. We find $\Delta s = 17 \mu\text{m}$ for the 80 Hz trap and $27 \mu\text{m}$ for the 200 Hz trap. Using a straightforward analysis, we estimate that the number of interfering pancakes, P , is related to Δs and the TOF, T , via $P = 2hT/(m \Delta s \lambda)$. From this we find $P = 20$ and 10 pancakes for the 80 Hz and 200 Hz traps, respectively. These numbers agree reasonably well with our measurements of the size of the BEC in the respective magnetic traps.

In conclusion, we have demonstrated the 1-D Mott insulator transition by applying a 1-D optical lattice to a BEC. We used Kapitza-Dirac scattering as an accurate way to calibrate our lattice depth. We examined time-of-flight images of the BEC as a function of lattice depth, and found that the BEC is fully in the Mott insulator state at $30 E_{\text{rec}}$, and requires a certain time to dephase. Furthermore, we observe random interference patterns in time-of-flight images, providing evidence that the 1-D Mott insulator consists of pancake BECs that still retain superfluid properties, including a definite phase.

We acknowledge the support of AFOSR grant FA9550-07-1-0412 and FOCUS (NSF grant PHY-0114336), as well as helpful discussions with Professor Luming Duan.

-
- [1] M. H. Anderson *et al.*, Science **269**, 198 (1995).
[2] K.B. Davis *et al.*, Phys. Rev. Lett. **75**, 3969 (1995).
[3] M. Greiner *et al.*, Nature **415**, 39 (2002).
[4] K. Goral, L. Santos, and M. Lewenstein, Phys. Rev. Lett. **88**, 170406 (2002).
[5] S. Ospelkaus *et al.*, Phys. Rev. Lett. **96**, 180403 (2006).
[6] T. Rom *et al.*, Phys. Rev. Lett. **93**, 073002 (2004).
[7] D. Jaksch *et al.*, Phys. Rev. Lett. **89**, 040402 (2002).
[8] M. G. Moore and H. R. Sadeghpour, Phys. Rev. A **67**, 041603(R) (2003).
[9] D. Jaksch, Contemporary Physics **45** 367-381 (2004)
[10] K. Xu *et al.*, Phys. Rev. A **72**, 043604 (2005).
[11] I. B. Spielman, W.D. Phillips, and J.V. Porto, Phys. Rev. Lett. **98**, 080404 (2007).
[12] M. Kohl *et al.*, J. Low Temp. Phys. **138**, 635 (2005).
[13] T. Stoferle *et al.*, Phys. Rev. Lett. **92** 130403 (2004).
[14] Jinbin Li *et al.*, arXiv:cond-mat/0311012v2 [cond-mat.soft] 7 Feb 2006.
[15] D. van Oosten, P. van der Straten, and H.T.C. Stoof, Phys. Rev. A **67**, 033606 (2003).
[16] In our work, the parameter V_{\perp} used in Ref. [13] is $V_{\perp} = 0$.
[17] R. Zhang, R. E. Sapiro, N. V. Morrow, R. R. Mhaskar, and G. Raithel, submitted.
[18] Roberto B. Diener *et al.*, Phys. Rev. Lett. **98** 180404

(2007)